



Technical Report

An experimental study on the ratcheting and fatigue behavior of polyacetal under uniaxial cyclic loading

Mahmoud Shariati*, Hossein Hatami, Hossein Yarahmadi, Hamid Reza Eipakchi

Department of Mechanical Engineering, Shahrood University of Technology, Shahrood, Iran

ARTICLE INFO

Article history:

Received 26 May 2011

Accepted 10 August 2011

Available online xxxx

Keywords:

Polymers

Fatigue

Plastic behavior

ABSTRACT

This paper presents an experimental study on the behavior of polyacetal or Polyoxymethylene (POM) under uniaxial cyclic loading. All experiments were performed in the stress-controlled mode. The tests were divided into nine groups, where different combinations of the mean stress or stress amplitude were used. Uniaxial fatigue or cyclic testing of polymeric materials is performed on specimens with geometry according to ASTM D638-03 or its equivalent, ISO 527-1. In this study, the diameter of the polyacetal test specimens was 20 mm. The specimens were prepared using a CNC lathe. The gage length of the specimens was 30 mm, and the diameter of the specimens was 10.1 mm. The stress–strain data were recorded during each cycle of the experimental tests. Based on the obtained stress–strain data, quantitative analysis of the mechanical parameters were done in which the strain ratcheting, strain range, strain energy density and the slope of the stress–strain hysteresis loops were calculated. The experimental data showed that the ratcheting strain and strain rate ratcheting are sensitive to the applied stress amplitude and the mean stress. Mean stress functions were used in the equivalent damage parameter and included the mean stress effect on the fatigue life of the polyacetal. The material constants were calibrated using the stress, strain and energy approaches. Finally, it was found that the stress and energy approaches were more successful in predicting the fatigue life of polyacetal.

© 2011 Elsevier Ltd. All rights reserved.

1. Introduction

Ratcheting is a kind of special cyclic deformation behavior that occurs in materials and structures subjected to cyclic stressing with a non-zero mean stress, where the stresses are greater than the material's yield stress. Thus, the materials or structures will yield under the applied loading. Ratcheting is particularly important in safety and fatigue life prediction of engineering structures because many types of structures are subjected to cyclic loading, where the applied stress exceeds the yield stress of the used material. For the design and analysis of these types of structures, accurately predicting the ratcheting response is critical because ratcheting can lead to catastrophic failure of the structures. Even for structures that are designed to behave in the elastic limit, plastic zones may exist at the discontinuities or at the tip of cracks, and fatigue cracks can initiate at the plastic zones. Therefore, an accurate simulation that models the cyclic plasticity response is important in predicting the high-cycle fatigue life as well [1]. In the last two decades, the ratcheting phenomena has been extensively studied by experiments and simulations.

Several studies have investigated the ratcheting behavior of metallic materials. For example, Kim et al. studied the fatigue and the ratcheting of a type of copper alloy [2]. Yang investigated the fatigue and ratcheting of carbon steel C45 [3]. Kang et al. studied the ratcheting and fatigue behavior of stainless steel SS304 [4]. Additionally, similar studies have been done in this field [5–8]. Such experimental tests and obtained data can help to better simulate and advance cyclic plasticity models and, thus, progress the analytical models on the ratcheting behavior of metals [9–12].

However, there are more studies on metallic materials than on polymeric materials in recent years; there have been only a few experimental tests performed that study the ratcheting behavior of polymeric materials. Among the studies that have focused on polymeric materials, Gang Tao and Zihui Xia studied a type of polymer [13,14]. Xu Chen and Shucai Hui studied the polymer, PTFE, and its ratcheting behavior under a compressive cyclic loading [15]. Other studies of polymeric materials have also been performed [16–22]. However, to improve the plasticity models for polymeric materials, more experimental data are required.

Due to the widespread applications of polyacetal, which is used to create bearings and gear types, and the lack of experimental data on the ratcheting behavior of polymeric materials, a study on the fatigue and ratcheting behavior of polyacetal is needed. Polyacetal, or POM, is an engineering polymer with a wide range of applications that exhibits mechanical properties similar to some metals. This

* Corresponding author. Tel.: +98 273 3395503; fax: +98 273 3391460.

E-mail addresses: mshariati@shahroodut.ac.ir, mshariati44@gmail.com (M. Shariati).

polymer, which was introduced to the polymer industry in 1960, has excellent mechanical properties that fill the space between ordinary polymers and metals. Applications of this polymer include use in the automotive industries, electrical equipment, construction, hardware and electronics. Polyacetal is almost a crystalline polymer that can be produced from polymerase formaldehyde ($-\text{CH}_2-\text{O}-$). Polyacetal is a competitor with the nylons (polyamides), which have several serious deficiencies, such as their poor dimensional stability in the presence of humidity. Because of their excellent molding ability, polyacetal resins are particularly useful when producing complex, industrial experimental components.

2. Specimens and test setup

Uniaxial fatigue or cyclic testing of polymeric materials is often performed on flat, dog bone-shaped specimens with a geometry according to ASTM D638-03 [23] or its equivalent, ISO 527-1 [24–27]. Because the diameters of the specimens in this study were quite small compared with their length, compressive loads could not be applied due to the risk of the specimens buckling, even at very low load levels. Fully reversed loading cycles can be applied if cylindrical specimens are used, where the specimen cannot be too slender to ensure that compressive loads can be applied without buckling. However, cyclic testing of polymers under fully reversed, uniaxial loading conditions is currently not a specified standard, and in the literature, a variety of cylindrical specimen sizes have been used, with different geometries and dimensions of gage length. In this study, the diameter of the polyacetal test specimens was 20 mm. The specimens were prepared using a CNC lathe. As seen in Fig. 1, the gage length of the specimens was 30 mm, and the diameter of the specimens was 10.1 mm.

The geometry of the used fixture is shown in Fig. 2.

The experimental device used in this study was a servo hydraulics INSTRON 8802 machine, as shown in Fig. 3.

3. Experimental procedure and results

To determine the mechanical properties of polyacetal, simple tension and standard compression tests were performed according to ASTM D638-03 standard test [23]. The obtained results are shown in Figs. 4 and 5, respectively.

Table 1 shows the mechanical properties of polyacetal obtained from the experimental tests.

All tests were performed in the stress-controlled condition at room temperature. The loading rate was maintained at 10 MPa/s for each test. So all fatigue tests were run at frequency less than $\omega = 1$ Hz (in the range of 0.04–0.125 Hz). It has been reported that interior temperature of polymer material would not rise markedly when the alternation frequency was less than or equal to 1 Hz, so the thermal effect during the fatigue was ignored in the paper [17]. The mean stress and stress amplitude applied in each test is given in Table 2.

Also, Table 2, shows the average values of the mechanical properties, (mean strain (ϵ_m^{avg}), strain amplitude (ϵ_a^{avg}), the dissipation

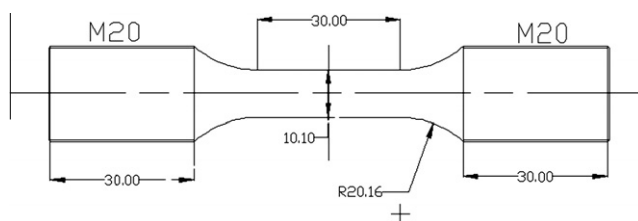


Fig. 1. Specimen geometry.

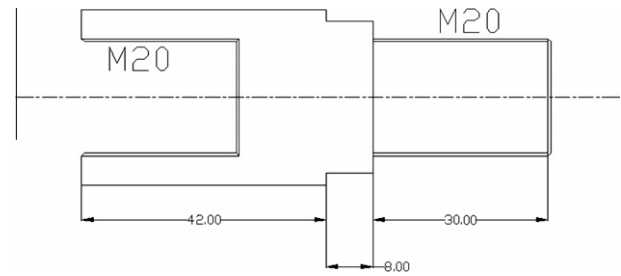


Fig. 2. Fixture geometry.



Fig. 3. Servo hydraulic INSTRON 8802 machine.

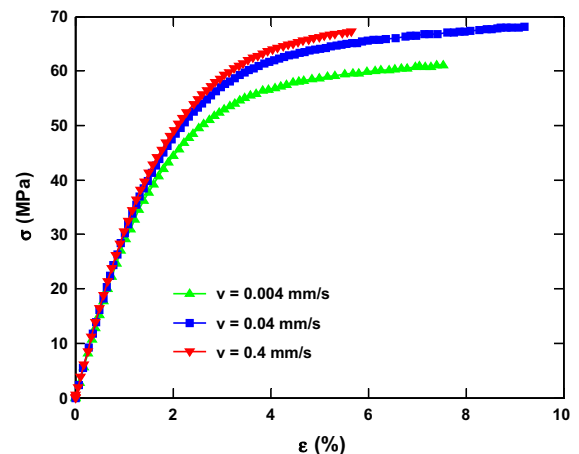


Fig. 4. Stress–strain curve of polyacetal under simple tension.

strain energy density (ΔW_{avg}^d) and the elastic strain energy density amplitude (ΔW_{avg}^e). To investigate the effect of varying the mean stresses (σ_m) and amplitude stresses (σ_a), nine tests were performed (GT1–GT9).

In groups GT1–GT5, the mean stress was constant, and the stress amplitude was variable. In groups GT6–GT9, the mean stress was variable, and the stress amplitude was constant. Thus, the effects of the loading in each experiment could be clearly distinguished. This grouping is given in Table 3.

The following sections will explain the quantitative analysis of the mechanical parameters, (stress range, the mean stress and the strain energy density) using the stress–strain data.

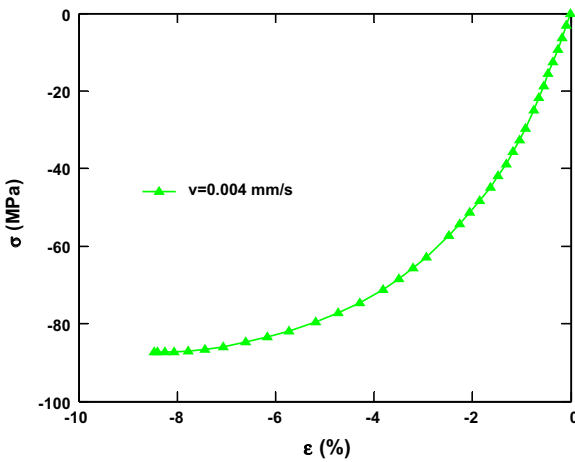


Fig. 5. Stress–strain curve of polyacetal under simple compression.

Table 1
Mechanical properties of polyacetal.

Mechanical properties	Tension	Compression
Modulus of elasticity (<i>E</i>)	3100 MPa	3400 MPa
Yield stress (σ_y)	39.9 MPa	–39.78 MPa
Yield strain (ϵ_y)	1.49%	–1.37%

3.1. Stress–strain hysteresis loops

Basic information from the cyclic behavior of a material can be obtained from the hysteresis loops of the stress–strain data. Cyclic deformation incurs a hysteresis loop for each cycle of the loading. For example, the hysteresis loops from the stress–strain tests, T2, T17 and T23, are shown in Fig. 6, and as can be seen, as the number of loading cycles (*N*) increased, the loop becomes fatter.

According to the definition of ratcheting, ratcheting strain occurs when the mean stress is non-zero. However, because the mechanical properties of polyacetal vary depending on the tension

Table 2
Experimental result.

Test	σ_m (MPa)	σ_a (MPa)	ϵ_m^{avg} (%)	ϵ_a^{avg} (%)	ΔW_{avg}^d (KJ/m ³)	ΔW_{avg}^e (KJ/m ³)	<i>N_f</i>
T1	0.00	60.63	1.21	3.51	790.4	978.4	46
T2	0.00	53.87	0.47	3.09	545.5	748.1	159
T3	0.00	47.11	0.37	2.50	300.8	550.1	566
T4	0.00	40.35	0.14	1.98	149.4	364.6	3312
T5	33.59	30.21	3.14	2.08	357.3	236.7	32
T6	33.59	26.83	3.94	1.81	195.3	193.7	306
T7	33.59	23.45	4.84	1.53	111.2	148.2	1556
T8	33.59	20.07	5.48	1.09	42.8	100.1	26,678
T9	30.21	33.59	3.20	2.44	554.5	319.8	64
T10	30.21	30.21	3.31	2.11	284.6	239.0	204
T11	30.21	26.83	3.55	1.89	198.7	199.3	302
T12	30.21	23.45	4.68	1.57	106.7	156.7	3008
T13	30.21	20.07	5.39	1.04	27.8	80.9	180,930
T14	26.83	30.21	2.74	2.03	249.7	235.3	238
T15	26.83	26.83	2.76	1.69	149.8	191.1	796
T16	26.83	25.14	3.81	1.65	121.7	163.9	3264
T17	26.83	23.45	3.90	1.16	46.8	123.1	80,096
T18	23.45	30.21	2.36	1.88	195.1	228.7	596
T19	23.45	26.83	2.83	1.07	37.8	116.0	76,488
T20	28.52	23.45	4.28	1.43	82.2	151.5	12,458
T21	35.62	20.07	6.79	1.23	57.9	114.5	9944
T22	40.35	20.07	6.64	1.19	67.2	107.7	1962
T23	–16.69	43.73	–1.41	2.55	354.5	436.7	448
T24	–16.69	40.35	–1.30	2.22	249.8	354.8	1154
T25	–16.69	36.97	–2.13	2.06	195.8	315.0	36,784

Table 3
Categorize of tests.

Number of group	Mean stress	Stress amplitude	Number of tests
GT1	Constant	Variable	T1, T2, T3, T4
GT2	Constant	Variable	T5, T6, T7, T8
GT3	Constant	Variable	T9, T10, T11, T12, T13
GT4	Constant	Variable	T14, T15, T16, T17
GT5	Constant	Variable	T23, T24, T25
GT6	Variable	Constant	T5, T10, T14, T18
GT7	Variable	Constant	T6, T11, T15, T19
GT8	Variable	Constant	T7, T12, T20, T17
GT9	Variable	Constant	T22, T21, T8, T13

and the pressure, some ratcheting strain was seen when the mean stress was zero (Fig. 6-T2), though the strain was much less than that in the case of the non-zero mean stress.

3.2. Changes in the ratcheting strain

The ratcheting strain (ϵ_r) can be obtained from the incremental peak strain of the hysteresis loop after each cycle (Eq. (1)).

$$\delta\epsilon = \epsilon_{n+1}^{peak} + \epsilon_n^{peak} \tag{1}$$

However, the ratcheting strain can be defined as the mean strain of each cycle. Eq. (2) is the mathematical expression of this definition, and in this study, this relationship for the ratcheting strain was used. The ratcheting strain for the GT1–GT9 groups are shown in Fig. 7.

$$\epsilon_r = \frac{1}{2} (\epsilon_{max} + \epsilon_{min}) \tag{2}$$

3.3. Changes in the strain range

Fig. 8 shows the changes in the strain range during the stress-controlled tests for the constant mean stress and the variable stress amplitude.

As seen from the results, as the number of cycles increased, the changes in the strain range increased. Additionally, note that

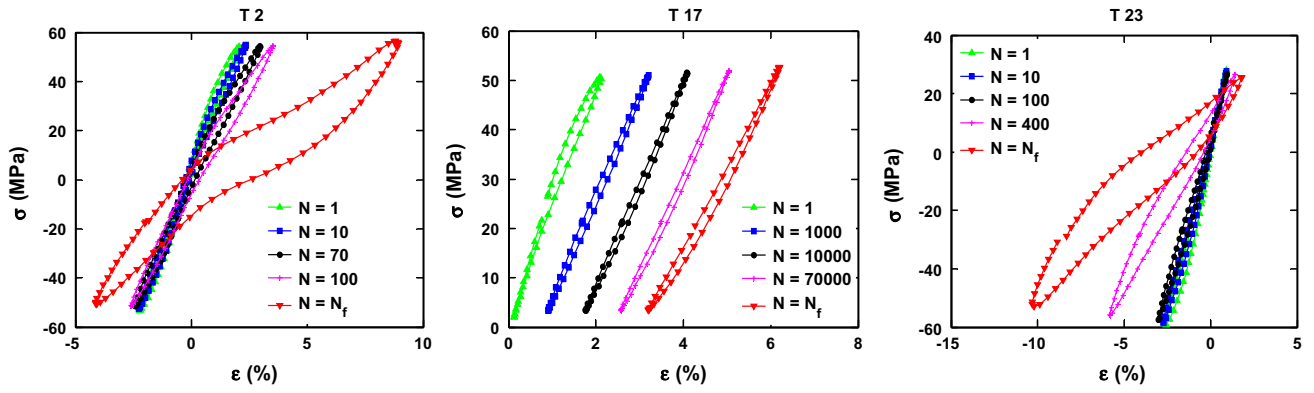


Fig. 6. Hysteresis loops of T2, T17, T23.

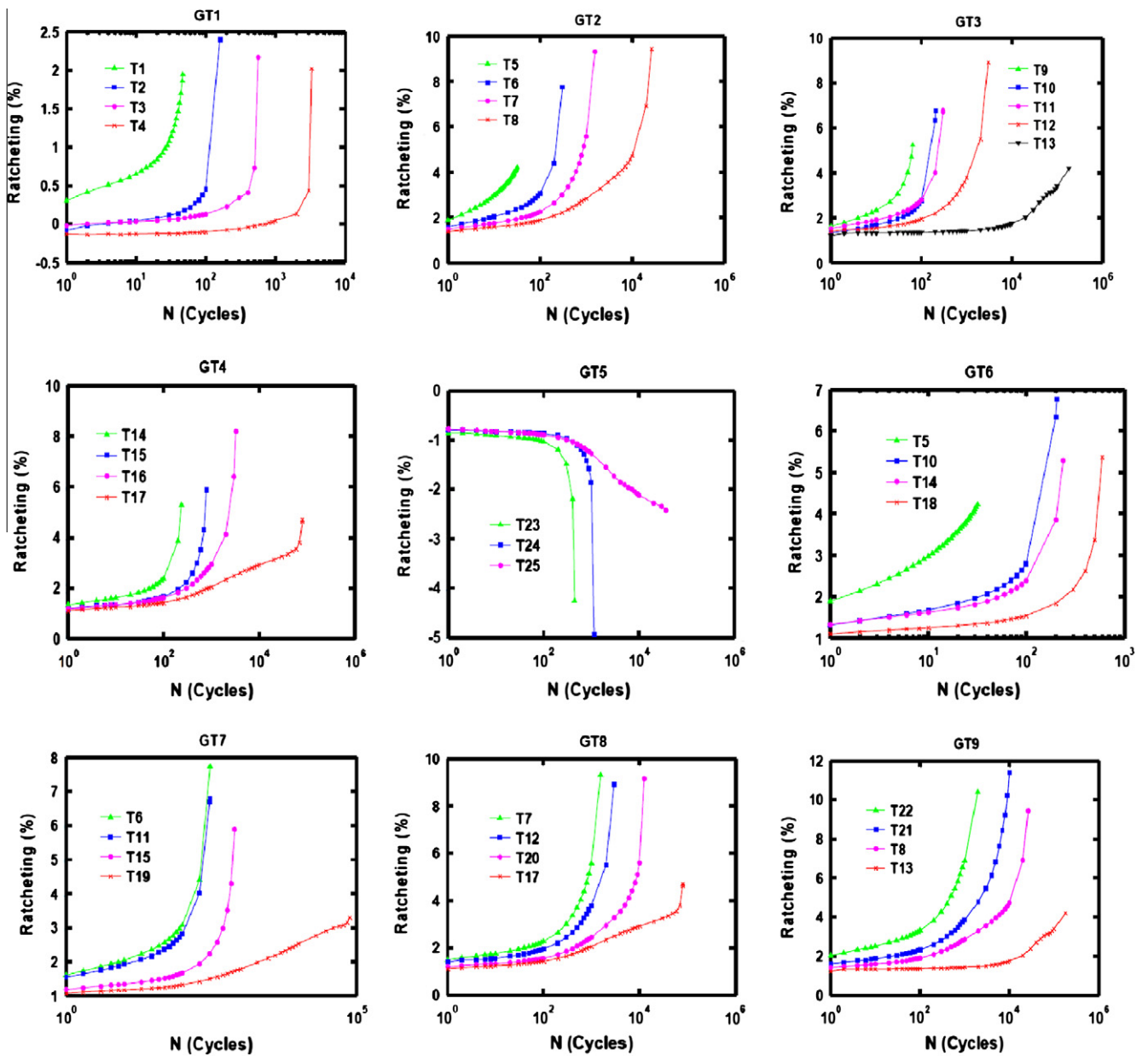


Fig. 7. The ratcheting strain for the GT1–GT9 groups.

in the low cycle fatigue, the rate of the changes of the strain range was greater than the strain range changes in the high cycle fatigue.

However, in the experiments with the variable stress amplitude and the constant mean stress, the amplitude of the applied stress on a specimen was larger, and the rate of the strain range changes was larger as well. Similarly, for the experiments with the constant stress amplitude and the variable mean stress, the applied mean stress on the specimen was larger, and the rate of the strain range was larger (Fig. 8).

3.4. Changes in the strain energy

In the fatigue field, two types of strain energy density are discussed. One type is called the dissipation strain energy density,

DSED or ΔW^d , and the other is called the elastic strain energy density amplitude, ESEDA or ΔW^e [13].

Based on the obtained stress-strain and hysteresis loops data, ΔW^d and ΔW^e can be calculated by integrating the corresponding areas, as shown in Fig. 9.

Both types of strain energy were calculated. According to Fig. 10, it is clear that for all the experimental groups (GT2–GT9), the DSED value decreased initially and then increased. As seen in the GT1 group test, where the mean stress was zero, the dissipation strain energy density either remained constant or increased. Any applied stress amplitude in the case of the zero mean stress was less steep, where the dissipation strain energy density increased less; so that in test T4, the rate of the change in the strain energy density reached zero.

An interesting point is that in the case of the non-zero mean stress and for each stress range value, the rate of change in the

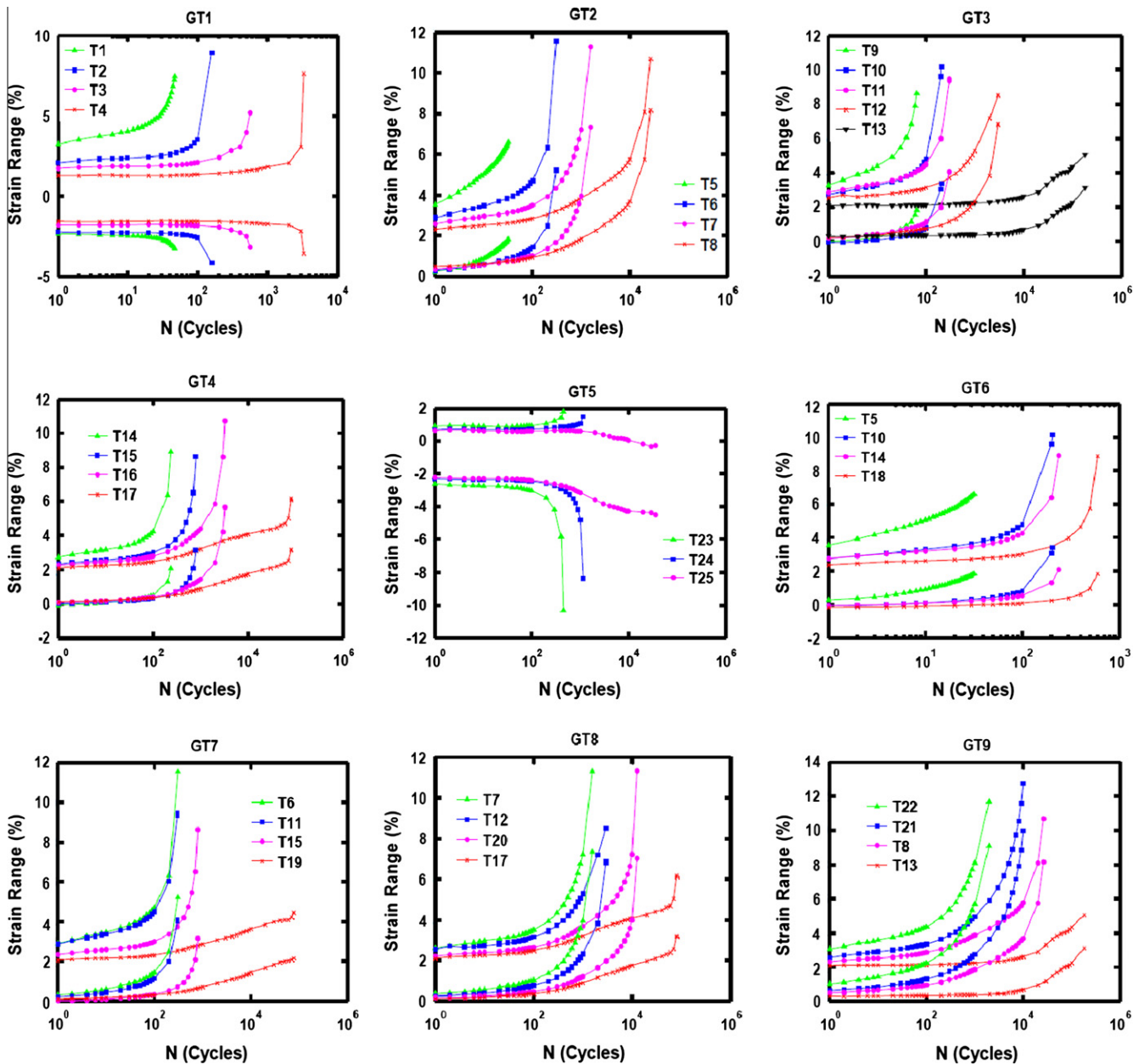


Fig. 8. The changes in the strain range for the GT1–GT9 groups.

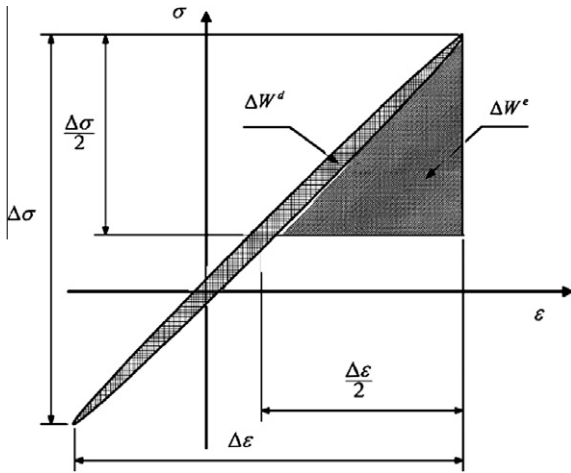


Fig. 9. Components of strain energy density [13].

dissipation strain energy density was initially negative, then zero and, finally, positive.

Fig. 11 illustrates the elastic strain energy density amplitude. As seen, the rate of change in the elastic strain energy density range was positive, but its behavior was very irregular.

3.5. Slope changes in the hysteresis loops

In this section, the parameter that was introduced in Ref. [17] is considered. This parameter, the hysteresis loop slope (E), is the gradient of the line that connects the extreme points of the hysteresis loops together. Fig. 12 shows this parameter symbolically.

From Fig. 13, it can be seen that the rates of the change in the slope of the hysteresis loops for the GT1–GT5 groups were always negative; however, the range of the applied stress on the specimen was greater, where the gradient lessened and decreased significantly. In the GT6–GT9 tests, where the stress amplitude and the mean stress were variable, increasing the applied stress on the specimen resulted in the hysteresis loop gradient being low, and the rate of changes of the hysteresis loops gradient increased.

4. Fatigue

Experimental fatigue tests were grouped into two categories: stress-controlled and strain-controlled fatigue experiments. If the material behaved elastically, the results of these tests were equivalent to each other; however, if the material behaved in the elastic–plastic range, the results were quite different from each other. In the stress-controlled experiments, the mean stress could lead to an accumulation of plastic strain in each cycle, which is called the ratcheting strain. Ratcheting strain can cause more damage and shorten the fatigue life. In the strain-controlled experiments, in the early stages, the mean stress relaxation occurred and thus, therefore reduced the mean stress effects on the fatigue life. In general, the theories for the fatigue life of structures, depending on their vision, can be divided in three categories: fatigue based on stress, fatigue based on strain and fatigue based on energy [27].

In each of the three approaches, the relationship between the amount of damage and the general fatigue life is generally expressed using the following formula:

$$\psi = \kappa \cdot (N_f)^\gamma + \psi_0 \quad (3)$$

where ψ is the damage parameter, N_f is the fatigue life, κ , γ are material constants and ψ_0 is the fatigue limit. However, depending

on the damage parameter selected, which could be a function of the stress, strain or strain energy, the fatigue analysis can be analyzed with either the stress, strain or energy. Each of the aforementioned approaches and their method of analyzing the fatigue life of polyacetal under stress-controlled tests will be explained.

4.1. Fatigue based on the stress approach

From Ref. [28], a simple power law function for the mean stress can be expressed as follows:

$$f\left(\frac{\sigma_m}{\sigma_a}\right) = \left(1 + \eta \frac{\sigma_m}{\sigma_a}\right)^n \quad (4)$$

where n and η are material constants. It will be assumed that the mean stress is a function of the equivalent stress, σ_{eq} .

$$\sigma_{eq} = \left(1 + \eta \frac{\sigma_m}{\sigma_a}\right)^n \sigma_a \quad (5)$$

It should be noted that in fully reversed experiments, where $\sigma_m = 0$, Eq. (5) converts $\sigma_{eq} = \sigma_{-1}$, where the -1 represents the fully reversed test. Thus, in the fully reversed tests, the equivalent stress is the amplitude stress. Replacing σ_{-1} with σ_{eq} , Eq. (5) becomes the following:

$$\left(1 + \eta \frac{(\sigma_m/\sigma_{-1})}{(\sigma_a/\sigma_{-1})}\right)^n \frac{\sigma_a}{\sigma_{-1}} = 1 \quad (6)$$

The relations, σ_a/σ_{-1} and σ_m/σ_{-1} , were plotted using different material constants in Fig. 14. For the limiting case, when $\sigma_a/\sigma_{-1} \rightarrow 0$, we can see that for $n > 1$, $\sigma_m/\sigma_{-1} \rightarrow 0$, and for $0 < n < 1$, then $\sigma_m/\sigma_{-1} \rightarrow \infty$. Neither of these two behaviors are physically meaningful because when the stress amplitude, σ_a , is zero, the loading is in the static condition, and the mean stress, σ_m , should be related to the static mechanical properties of the materials, where σ_m/σ_{-1} should approach zero. Therefore, in this study, only the value $n = 1$ was considered [12]. Accordingly, Eq. (6) becomes Eq. (7).

$$\frac{\sigma_a}{\sigma_{-1}} + \eta \frac{\sigma_m}{\sigma_{-1}} = 1 \quad (7)$$

Eq. (7) can be written as Eq. (8), where $\sigma_r = \sigma_{-1}/\eta$ is a reference stress.

$$\frac{\sigma_a}{\sigma_{-1}} + \eta \frac{\sigma_m}{\sigma_{-1}} = 1 \quad (8)$$

The term, σ_r , in the Soderberg formula is the yield stress, σ_y , in the Goodman relation is the ultimate strength, σ_u and in the Morrow's formula is the fatigue strength coefficient. Based on the suggestion from Zihui Xia and Gang Tao, for polymeric materials, σ_r should be a function of σ_{-1} [12]. In our case, η was taken to be an implicit constant, and we assumed that σ_r was a linear function of σ_{-1} . Generally, based on Eq. (3), we can consider a relationship between the equivalent stress, σ_{-1} , and the fatigue life as following a power law equation [12]:

$$\sigma_{eq} = \kappa \cdot N_f^\gamma + \sigma_0 \quad (9)$$

As mentioned before, if testing was performed completely fully reversed, then $\sigma_{eq} = \sigma_{-1} = \sigma_a$. Thus, Eq. (9) can be written as $\sigma_{eq} = \sigma_a = \kappa \cdot N_f^\gamma + \sigma_0$. By fitting a curve, we can find the values of κ , γ , σ_0 . Then Eq. (9) becomes Eq. (10).

$$\sigma_{eq} = 103.7N_f^{-0.461} + 40.93 \quad (10)$$

After determining the coefficients, κ , γ , σ_0 , for the tests, where there is non-zero mean stress, the fatigue life can be placed on the right side of Eq. (10), and the equivalent stress can be determined. Now, from Eq. (5), we have the following:

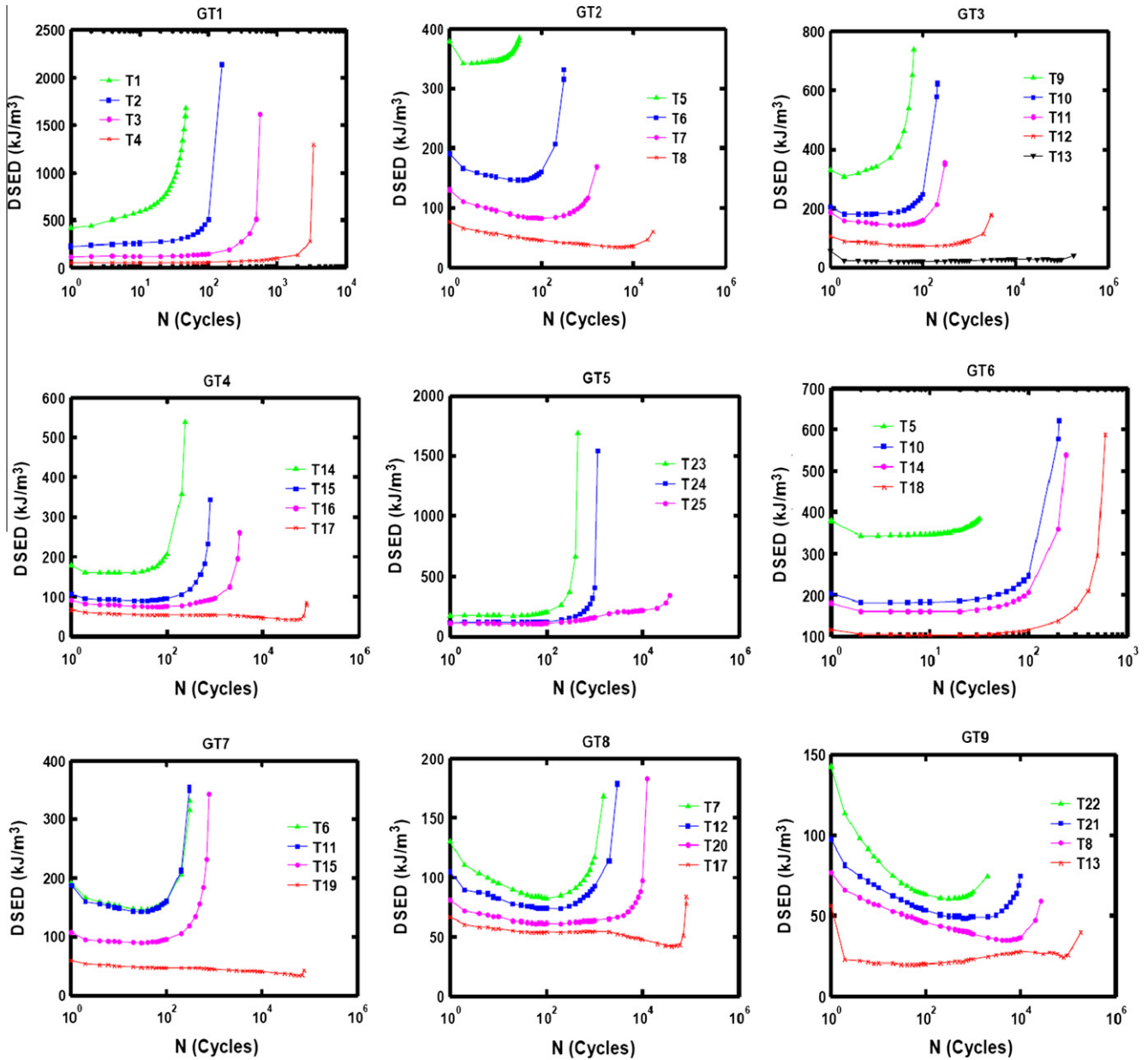


Fig. 10. The change in the dissipation strain energy density.

$$\frac{\sigma_a}{\sigma_{eq}} = \frac{1}{f\left(\frac{\sigma_m}{\sigma_a}\right)} \quad (11)$$

According to the aforementioned discussions, we have the following:

$$f\left(\frac{\sigma_m}{\sigma_a}\right) = 1 + \eta \frac{\sigma_m}{\sigma_a} \quad (12)$$

Combining Eqs. (11) and (12) results in, Eq. (13).

$$\sigma_{eq} = \left(1 + \eta \frac{\sigma_m}{\sigma_a}\right) \sigma_a \quad (13)$$

By fitting a curve from the data to σ_{eq}/σ_a vs. σ_m/σ_a , as seen in Fig. 15, η was determined to be 0.655.

Therefore, predicting the fatigue life of the polyacetal using a stress-controlled approach can be determined using Eq. (14).

$$\left(1 + 0.655 \frac{\sigma_m}{\sigma_a}\right) \sigma_a = 103.7N_f^{-0.461} + 40.93 \quad (14)$$

This equation and the experimental test results are shown in Fig. 16.

4.2. Fatigue based on the strain approach

Another approach to analyze the fatigue life is the strain approach, which predicts the equivalent strain using the following equation:

$$\varepsilon_{eq} = \left(1 + \eta \frac{\varepsilon_m}{\varepsilon_a}\right) \varepsilon_a \quad (15)$$

during the stress-controlled tests, the mean strain and the strain amplitude values are not constant. Here, the mean strain is the ratcheting strain and is variable. Thus, in this study, the average values of the mean strain and strain amplitude are used for the fatigue

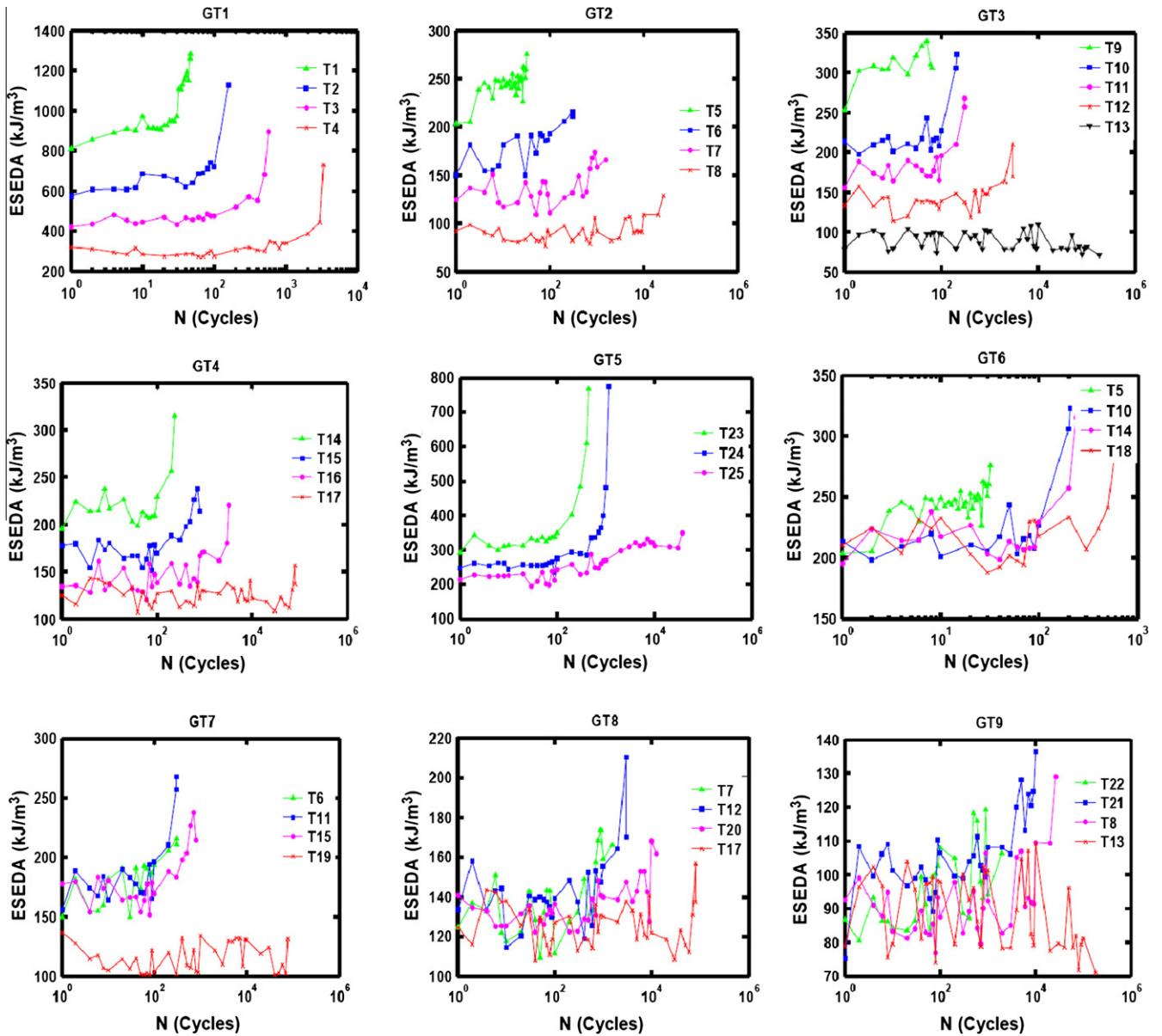


Fig. 11. The change in the elastic strain energy density amplitude.

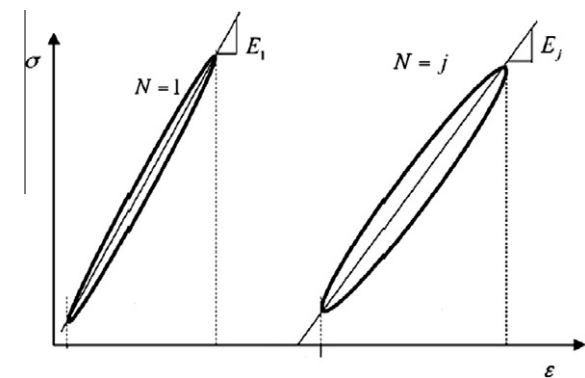


Fig. 12. The hysteresis loop slope [17].

calculations. Also according to Eq. (15), for the fully reversed tests (GTI test group), the value, ϵ_m , must equal zero until $\epsilon_{eq} = \epsilon_a$, whereas

for the GT1 test group, ϵ_m is not zero because, compared with the other test groups, ϵ_m is negligible for the GTI test group. Thus, in this study, ϵ_m was zero. The reason for the non-zero value of ϵ_m for the fully reversed tests is due to the non-linear behavior between the stress and the strain of polyacetal and also because of the non-symmetric tensile and compression loading behaviors. To study the fatigue from the perspective of the strain, we can consider the following equation for the equivalent strain:

$$\epsilon_{eq} = \epsilon_{-1} = \kappa \cdot N_f^\gamma + \epsilon_0 \tag{16}$$

By fitting a curve to the data points from the GTI test group, Eq. (16) is converted to Eq. (17).

$$\epsilon_{eq} = 9.921 N_f^{-0.421} + 1.7 \tag{17}$$

Therefore, the obtained values of the κ , γ , ϵ_0 parameters were 9.921, -0.421, and 1.7, respectively.

Now, using Eq. (17) and placing the fatigue life of each test instead on the right side of this equation, we can calculate ϵ_{eq} .

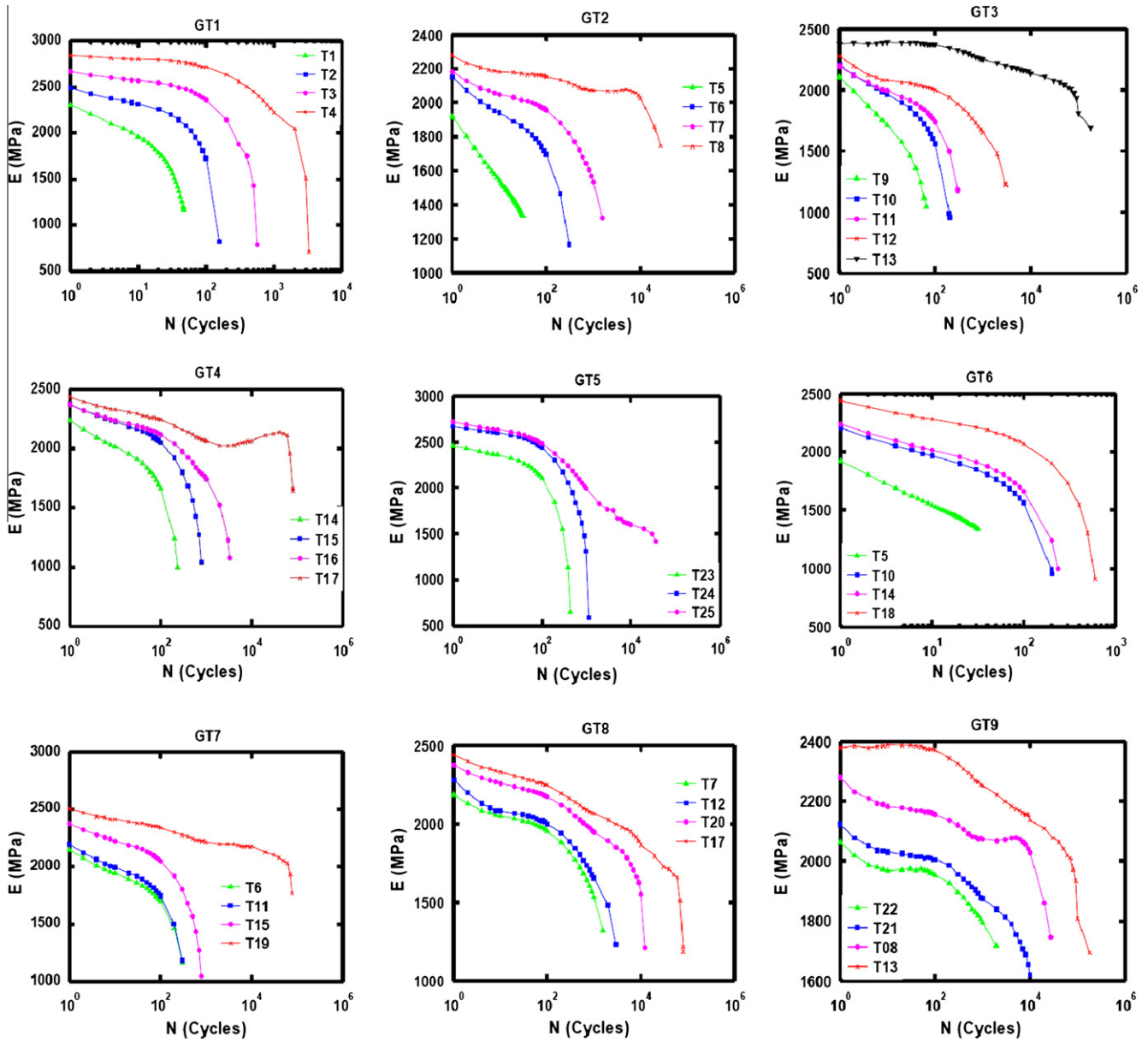


Fig. 13. The change in the slope of the hysteresis loops.

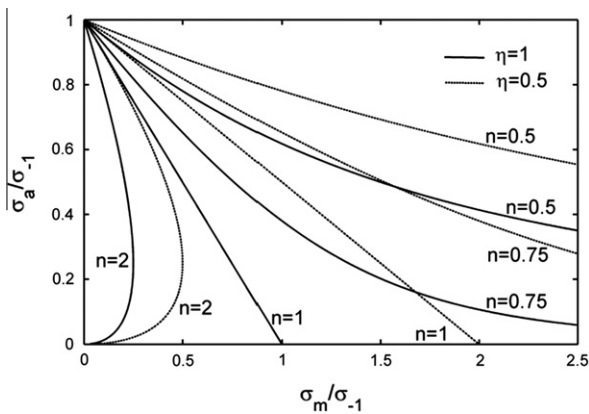


Fig. 14. Function of mean stress with different material constants [13].

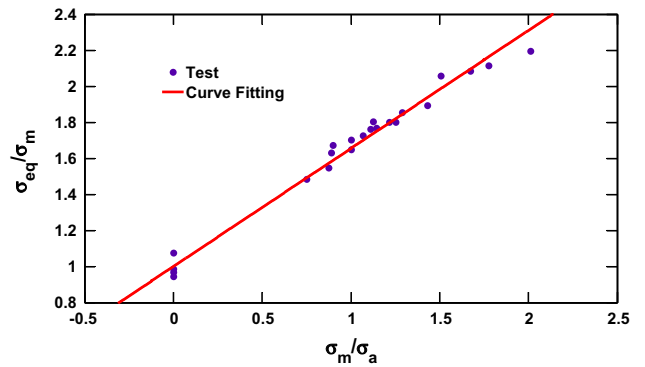


Fig. 15. Function of mean stress based on the stress approach.

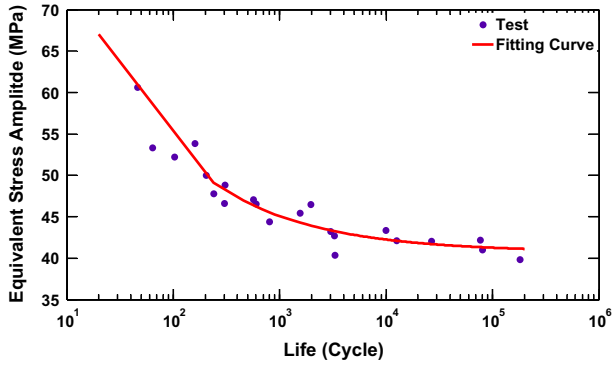


Fig. 16. Equivalent stress amplitude vs. fatigue life.

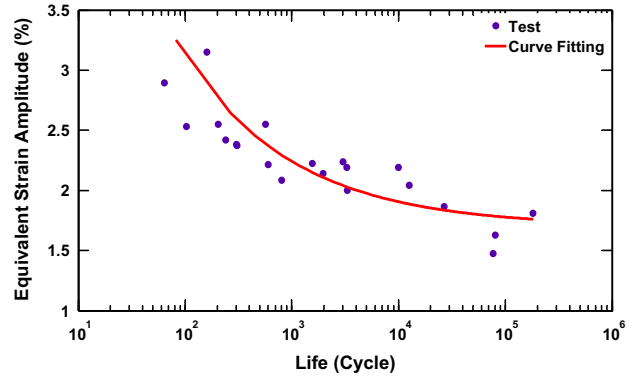


Fig. 18. Equivalent strain amplitude vs. fatigue life.

$$f\left(\frac{\epsilon_m}{\epsilon_a}\right) = 1 + \eta \frac{\epsilon_m}{\epsilon_a} \quad (18)$$

By calculating ϵ_{eq} and plotting the ϵ_{eq}/ϵ_a vs. ϵ_m/ϵ_a , Fig. 17 shows the fitted line as described by Eq. (18), where η was determined to be 0.143.

Using the determined η and Eq. (15), we once again calculate ϵ_{eq} , where the results vs. the fatigue life of each experiment are shown in Fig. 18. Thus, the relationship between the fatigue life of the stress- controlled tests using the strain approach was achieved.

$$\left(1 + 0.143 \frac{\epsilon_m}{\epsilon_a}\right) \epsilon_a = 9.921 N_f^{-0.421} + 1.7 \quad (19)$$

4.3. Fatigue based on the energy approach

The strain energy approach is different from the previous two approaches because before, the stress or strain approach calculations were based on only one quantity. For example, in the stress approach, the calculations were based on only the stress value, and the strain values did not affect the results. This approach is appropriate when the materials exhibit linear stress–strain behavior (like metals); however, when the stress–strain behavior is non-linear, such as with polymeric materials, more than one quantity is needed, so the energy approach is superior than the other two approaches because both the stress and the strain quantities are used in the calculations.

Using the energy approach, the mean stress function can be written as Eq. (20). Similar to the previous two stress and strain approaches, a relationship for the total energy associated with the fatigue life can be obtained (Eq. (21)).

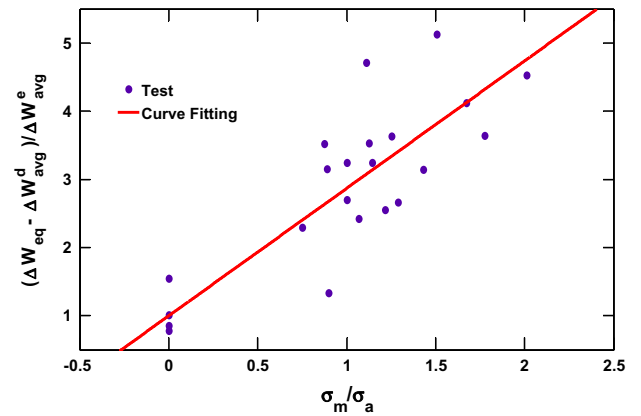


Fig. 19. Function of mean stress based on the energy approach.

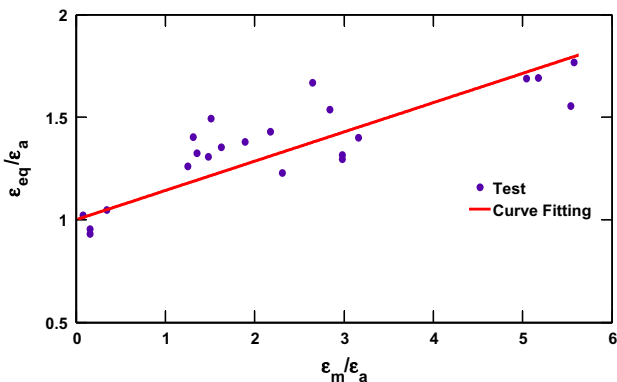


Fig. 17. Function of mean strain based on the strain approach.

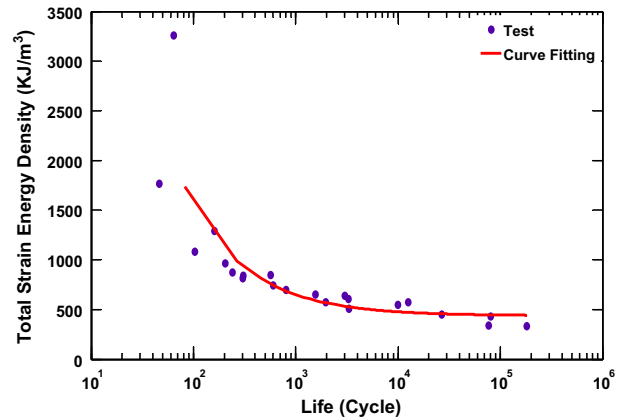


Fig. 20. Total strain energy density vs. fatigue life.

$$\Delta W_{eq} - \Delta W_{avg}^d = \left(1 + \eta \frac{\sigma_m}{\sigma_a}\right) \Delta W_{avg}^e \quad (20)$$

$$\Delta W_{eq} = \Delta W_{-1avg}^d + \Delta W_{-1avg}^e = \kappa \cdot N_f^\gamma + \Delta W_0 \quad (21)$$

Using the results from the fully reversed tests and Eq. (21), a curve can be fitted to the data points from the tests. Thus, the unknown coefficients of Eq. (21) can be obtained. Therefore, the equation is as follows:

$$\Delta W_{eq} = 31350 N_f^{-0.747} + 438 \quad (22)$$

Now, using the relations in Eq. (22), the values of ΔW_{eq} can be calculated for each test, where Fig. 19 shows the plot, $(\Delta W_{eq} - \Delta W_{avg}^d) / \Delta W_{avg}^d$ vs. σ_m / σ_a . By fitting a line from the points, η , as defined in Eq. (21), was determined to be 1.868. Using η and Eq. (20), the values of ΔW_{eq} were calculated, and Fig. 20 shows the draw vs. fatigue life.

By comparing the predicted results with the obtained results from the stress, strain and energy approaches, it is clear that the energy and stress approaches performed better than the strain approach.

5. Conclusions

In this study, stress-controlled tests on polyacetal were performed at laboratory ambient temperature, where different combinations of the mean stress and stress amplitude were used. Mechanical parameters, such as the strain range, the ratcheting strain, the slope of the hysteresis loops and the strain energy density, were investigated. The following results were obtained from this study.

- (1) By reducing the applied stress amplitude and the constant mean stress, the ratcheting strain rate decreased.
- (2) By reducing the applied mean stress and the constant stress amplitude, the ratcheting strain rate decreased.
- (3) Generally, reducing the stress amplitude and the mean stress constant resulted in the ratcheting strain decreasing.
- (4) Generally, reducing the mean stress with constant stress amplitude resulted in the ratcheting strain decreasing.
- (5) The stress and energy approaches were more successful in predicting the fatigue life of polyacetal.

References

- [1] Kang G. Ratchetting: recent progresses in phenomenon observation, constitutive modeling and application. *Int J Fatigue* 2008;30:1448–72.
- [2] Lim C-B, Kim KS, Seong JB. Ratcheting and fatigue behavior of a copper alloy under uniaxial cyclic loading with mean stress. *Int J Fatigue* 2009;31:501–7.
- [3] Yang X. Low cycle fatigue and cyclic stress ratcheting failure behavior of carbon steel 45 under uniaxial cyclic loading. *Int J Fatigue* 2005;27:1124–32.
- [4] Kang G, Liu Y, Li Zh. Experimental study on ratchetting-fatigue interaction of SS304 stainless steel in uniaxial cyclic stressing. *Mater Sci Eng A* 2006;435–436:396–404.
- [5] Nip KH, Gardner L, Davies CM, Elghazouli AY. Extremely low cycle fatigue tests on structural carbon steel and stainless steel. *J Constr Steel Res* 2010;66:96–110.
- [6] Gao H, Chen X. Effect of axial ratcheting deformation on torsional low cycle fatigue life of lead-free solder Sn–3.5Ag. *Int J Fatigue* 2009;31:276–83.
- [7] Chen G, Shan S-C, Chen X, Yuan H. Ratcheting and fatigue properties of the high-nitrogen steel X13CrMnMoN18–14–3 under cyclic loading. *Comput Mater Sci* 2009;46:572–8.
- [8] Chen X, Yu D-H, Kim KS. Experimental study on ratcheting behavior of eutectic tin–lead solder under multiaxial loading. *Mater Sci Eng A* 2005;406:86–94.
- [9] Kang G. A visco-plastic constitutive model for ratcheting of cyclically stable materials and its finite element implementation. *Mech Mater* 2004;36:299–312.
- [10] Chen X, Jiao R, Kim KS. On the Ohno–Wang kinematic hardening rules for multiaxial ratcheting modeling of medium carbon steel. *Int J Plast* 2005;21:161–84.
- [11] Colak OU. Kinematic hardening rules for modeling uniaxial and multiaxial ratcheting. *Mater Des* 2008;29:1575–81.
- [12] Abdel-Karim M. Modified kinematic hardening rules for simulations of ratchetting. *Int J Plast* 2009;25:1560–87.
- [13] Tao G, Xia Z. Mean stress/strain effect on fatigue behavior of an epoxy resin. *Int J Fatigue* 2007;29:2180–90.
- [14] Tao G, Xia Z. Ratcheting behavior of an epoxy polymer and its effect on fatigue life. *Polym Test* 2007;26:451–60.
- [15] Chen X, Hui S. Ratcheting behavior of PTFE under cyclic compression. *Polym Test* 2005;24:829–33.
- [16] Zhang Z, Chen X. Multiaxial ratcheting behavior of PTFE at room temperature. *Polym Test* 2009;28:288–95.
- [17] Liu W, Gao Z, Yue Z. Steady ratcheting strains accumulation in varying temperature fatigue tests of PMMA. *Mater Sci Eng A* 2008;492:102–9.
- [18] Bles G, Gadaj SP, Nowacki WK, Tourabi A. Experimental study of a PA66 solid polymer in the case of cyclic shear loading. *Arch Mech* 2002;54:155–74.
- [19] Avanzini A. Mechanical characterization and finite element modelling of cyclic stress–strain behaviour of ultrahigh molecular weight polyethylene. *Mater Des* 2008;29:330–43.
- [20] Ramkumar A, Gnanamoorthy R. Axial fatigue behaviour of polyamide-6 and polyamide-6 nanocomposites at room temperature. *Compos Sci Technol* 2008;68:3401–5.
- [21] Mallick PK, Zhou Y. Effect of mean stress on the stress-controlled fatigue of a short E-glass fiber reinforced polyamide-6,6. *Int J Fatigue* 2004;26:941–6.
- [22] Tao G, Xia Z. Biaxial fatigue behavior of an epoxy polymer with mean stress effect. *Int J Fatigue* 2009;31:678–85.
- [23] ASTM D 638-03. American society for testing materials. Standard test method for tensile properties of plastics. Philadelphia, USA; 2004.
- [24] NF EN ISO 527-1. International organization for standardization, plastics. Determination of tensile properties. Geneva, Switzerland; 1993.
- [25] Meyer RW, Pruitt LA. The effect of cyclic true strain on the morphology, structure, and relaxation behavior of ultrahigh molecular weight polyethylene. *Polymer* 2001;42:5293–306.
- [26] Niinomi M, Wang L, Enjitsu T, Fukunaga K. Fatigue characteristics of ultrahigh molecular weight polyethylene with different molecular weight for implant material. *J Mater Sci Mater Med* 2001;12:267–72.
- [27] Urries I, Medel FJ, Rios R, Gomez-Barrena E, Puertolas JA. Comparative cyclic stress–strain and fatigue resistance behavior of electron-beam- and gamma-irradiated ultrahigh molecular weight polyethylene. *J Biomed Mater Res Part B Appl Biomater* 2004;70B:152–60.
- [28] Kujawski D, Ellyin F. A unified approach to mean stress effect on fatigue threshold conditions. *Int J Fatigue* 1995;17:101–6.